

# Effects of irradiation on radioresistance, HOTAIR and epithelial-mesenchymal transition/cancer stem cell marker expression in esophageal squamous cell carcinoma

CHUNLI DA<sup>1</sup>, LI WU<sup>1</sup>, YUTING LIU<sup>2</sup>, RUOZHENG WANG<sup>1</sup> and RUIGUANG LI<sup>3</sup>

<sup>1</sup>Radiotherapy Center; <sup>2</sup>Department of Anesthesiology and <sup>3</sup>Endoscopic Diagnosis and Treatment Center, Affiliated Tumor Hospital of Xinjiang Medical University, Urumqi, Xinjiang 830000, P.R. China

Received October 22, 2015; Accepted September 22, 2016

DOI: 10.3892/ol.2017.5774

**Abstract.** Radiotherapy is a common therapeutic strategy used to treat esophageal squamous cell carcinoma (ESCC). However, tumor cells often develop radioresistance, thereby reducing treatment efficacy. Here, we aimed to identify the mechanisms through which ESCC cells develop radioresistance and identify associated biomarkers. Eca109 cells were exposed to repeated radiation at 2 Gy/fraction for a total dose of 60 Gy (Eca109R60/2Gy cells). MTT and colony formation assays were performed to measure cell proliferation and compare the radiation biology parameters of Eca109 and Eca109R60/2Gy cells. Cell cycle distributions and apoptosis were assessed by flow cytometry. Reverse transcription-quantitative polymerase chain reaction and western blotting were employed to analyze the expression of HOX transcript antisense RNA (HOTAIR), in addition to biomarkers of the epithelial-mesenchymal transition (EMT) and cancer stem cells (CSCs). Eca109R60/2Gy cells exhibited increased cell proliferation and clone formation, with significantly higher radiobiological parameters compared with the parental Eca109 cells. The Eca109R60/2Gy cells also exhibited significantly decreased accumulation in G<sub>2</sub> phase and increased accumulation in S phase. Additionally, the apoptosis rate was significantly lower in Eca109R60/2Gy cells than in parental Eca109 cells. Finally, *HOTAIR* expression

levels and *SNAIL* and  $\beta$ -catenin mRNA and protein expression levels were significantly higher, whereas E-cadherin levels were significantly lower in Eca109R60/2Gy cells than in Eca109 cells. Therefore, our findings demonstrated that radioresistance was affected by the expression of HOTAIR and biomarkers of the EMT and CSCs.

## Introduction

Esophageal carcinoma is one of the most common malignant diseases worldwide; in 2012, ~450,000 people (3.2% of all cancer cases) were diagnosed with esophageal cancer, and 400,000 patients (4.9% of the total) succumbed to of esophageal cancer-associated causes worldwide (1). There are two primary histological subtypes of esophageal cancer: Esophageal adenocarcinoma and esophageal squamous cell carcinoma (ESCC) (2). In China, ESCC is the predominant histological type (3). Radiotherapy is the primary treatment strategy for ESCC; however, the 5-year survival rate remains unsatisfactory at 10-20%, and the local recurrence rate is high (4). Recurrence primarily occurs due to the development of radioresistance in cancer cells following radiotherapy (5).

Currently, few clinical approaches are able to predict the effects of radiation therapy in patients with cancer or its effect on the radiosensitivity of cancer cells. Thus, identifying the mechanisms that promote ESCC radioresistance and the biomarkers involved in this process may facilitate the development of novel methods for predicting radiation efficiency and pharmacological strategies to improve the efficacy of radiation therapy.

Long noncoding RNAs (lncRNAs) are key regulatory RNAs that do not code for proteins and are crucial in various biological processes, including genomic imprinting, gene regulation, and chromatin organization (6-9). Additionally, several studies have demonstrated that multiple lncRNAs are associated with chromatin-modifying complexes, thereby affecting epigenetic information and conferring the properties required for chemotherapy resistance, tumor progression, and the metastatic phenotype (8,10).

HOX transcript antisense RNA (*HOTAIR*) is an lncRNA that is 2,158 bp long and is located on chromosome 12 within the homeobox C gene cluster (11). *HOTAIR* was originally

---

*Correspondence to:* Dr Ruozheng Wang, Radiotherapy Center, Affiliated Tumor Hospital of Xinjiang Medical University, 789 Suzhou East Street, New Urban Area, Urumqi, Xinjiang 830000, P.R. China  
E-mail: wrz8526@163.com

*Abbreviations:* ESCC, esophageal squamous cell carcinoma; EMT, epithelial-mesenchymal transition; CSC, cancer stem cell; RT-qPCR, reverse transcription-quantitative polymerase chain reaction; lncRNA, long noncoding RNA; TBST, Tris-buffered saline Tween-20

*Key words:* esophageal squamous cell carcinoma, Eca109, irradiation, radioresistance, HOX transcript antisense RNA, epithelial-mesenchymal transition, cancer stem cells

observed to be highly expressed in primary and metastatic breast cancer (6), suggesting that this lncRNA may affect tumor incidence, *in situ* invasion and distant metastasis. *HOTAIR* regulates metastatic progression in hepatocellular carcinoma (12); therefore, therapeutic targeting of this protein may reduce tumor recurrence. Additionally, *HOTAIR* may predict tumor recurrence following liver transplantation and could therefore function as a prognostic indicator (13). Furthermore, frequent upregulation of *HOTAIR* expression is associated with colorectal cancer (14,15), lung cancer (16), and other types of carcinoma. *HOTAIR* is expressed at higher levels in cancer with lymph node involvement and organ metastasis, and this higher level of expression is correlated with increased chemoresistance and mortality, in addition to a poorer prognosis (13,17). However, it remains unclear whether *HOTAIR* is involved in the development of radioresistance in human ESCCs.

Cancer stem cells (CSCs) are self-renewing, stem-like cancer cells and are the only subpopulation of cells within a tumor able to proliferate extensively, participate in the formation of metastases, and facilitate the development of chemo- or radioresistance (18,19). The epithelial-mesenchymal transition (EMT) generates cells with stem-like properties (20). Notably, *HOTAIR* regulates the expression of SNAIL (6), E-cadherin (14,15) and  $\beta$ -catenin (21). These three proteins are biomarkers of EMT and CSCs, thereby participating in tumor progression and subsequently resulting in poor patient prognosis. Previous studies have suggested a possible association between *HOTAIR*/EMT-associated factors and CSCs with chemotherapy resistance (13,17,22). However, no studies have yet linked *HOTAIR*, EMT-associated factors and CSCs with radioresistance in human malignancies, including esophageal cancer.

The present study aimed to elucidate the mechanisms mediating radioresistance in ESCC cells. Therefore, Eca109R60/2Gy cells were developed from parental Eca109 cells following the application of fractionated radiation (2 Gy), and the expression levels of *HOTAIR* and biomarkers of the EMT and CSCs were measured prior to and following radiation to investigate the roles of *HOTAIR*, EMT-associated factors, and CSCs in ESCC radioresistance.

## Materials and methods

**Cell culture.** The poorly-differentiated human Eca109 ESCC line was provided by Professor Huiwu Li from the Department of Biochemistry, Xinjiang Medical University (Urumqi, China). Cells were cultured in RPMI-1640 medium (Thermo Fisher Scientific, Inc., Waltham, MA, USA) supplemented with 10% fetal bovine serum (FBS; Sijiqing Biological Engineering Materials Co., Ltd., Hangzhou, China), 100 U/ml penicillin and 100 mg/ml streptomycin (Gino Biological Medicine Technology Co., Ltd., Hangzhou, China) at 37°C in a humidified atmosphere containing 5% CO<sub>2</sub>. Upon reaching confluence, cells were digested with pancreatin (Biyuntian Biological Technology Co. Ltd, Shanghai, China) and passaged.

**Construction of the radioresistant cell model.** During the exponential growth phase, Eca109 cells (at 50-60% confluence) were subjected to 2 Gy X-ray irradiation at a dose rate of

2.5 Gy/min using a Varian-6/100 Linear Accelerator (Varian Medical Systems, Inc., Palo Alto, CA, USA), and the culture medium was changed immediately following irradiation, using RPMI-1640 culture medium supplemented with 10% FBS. The culture medium was then changed every two days; if a large number of dead cells were observed, the amount of FBS was increased to 15%. Cells were cultured further in a humidified 5% CO<sub>2</sub> incubator and passaged after reaching a confluence of between 70 and 80%. This process was repeated until the total radiation dose reached 60 Gy. Cells resistant to 60 Gy radiation were designated Eca109R60/2Gy cells, and were cultured further for  $\geq 2$  weeks prior to subsequent experiments.

**MTT assay.** Eca109 and Eca109R60/2Gy cells were incubated at  $6 \times 10^3$  cells/100  $\mu$ l/well in 96-well plates. The wells at the edge of the plate were filled with 100  $\mu$ l PBS (Biochemical Products Co., Ltd, Beijing, China) as controls. A total of six replicate wells were used for each cell type. All wells were clearly marked according to designation, and the culture medium was changed every day for 7 days.

MTT assays were performed by adding 20  $\mu$ l MTT solution (5 g/l, Sigma-Aldrich; Merck Millipore, Darmstadt, Germany) to each well containing culture medium. The supernatant was discarded 4 h later, and 150  $\mu$ l dimethyl sulfoxide (DMSO; Sigma-Aldrich; Merck Millipore) was added. Once the formazan crystals had completely dissolved, the optical density (OD) was measured at 490 nm in a full wavelength microplate spectrophotometer (Thermo Fisher Scientific, Inc.), and growth curves were constructed.

**Plate colony formation assay.** Different densities of Eca109 or Eca109R60/2Gy cells were plated in 6-well plates (Table I), with three wells of cells used for each radiation dosage. All plated cells were agitated and subsequently incubated at 37°C in a humidified incubator with 5% CO<sub>2</sub> for 24 h to promote the attachment of cells to the plate. Cells were then irradiated with 0, 2, 4, 6, 8 or 10 Gy using X-ray irradiation and cultured for 8 days, at which point colonies could be identified by the naked eye. The cells were subsequently washed twice with PBS, fixed in 70% methanol for 15 min, and stained with 0.1% crystal violet for 15 min at room temperature (22°C). Colonies containing more than 50 cells were counted, and the clone formation efficiency was calculated as the ratio of clone numbers to plated cell numbers in each well.

**Flow cytometry assay.** For the analysis of cell cycle distribution, Eca109 or Eca109R60/2Gy cells were harvested, washed twice with PBS, and fixed with 70% cold ethanol at 4°C overnight. Cells were subsequently washed with PBS and incubated with RNase A at a final concentration of 50 mg/ml at 37°C for 30 min prior to centrifugation (5 min, 2-8°C, 110 x g). Cell pellets were resuspended and incubated with 50 mg/ml propidium iodide (PI) at room temperature for 30 min. Cell cycle distribution was analyzed using a flow cytometer (BD Biosciences, San Jose, CA, USA).

To analyze apoptosis, Eca109 or Eca109R60/2Gy cells were harvested and stained with Annexin V-fluorescein isothiocyanate (FITC)/PI for 15 min using an Annexin V-fluorescein isothiocyanate (FITC) Apoptosis Detection kit/Propidium Staining kit (BD Biosciences), according to

Table I. Cell densities at various radiation doses for the plate clone formation assay.

Irradiation dose (Gy)	Cell number (cells/plate)
0	100
2	500
4	1,000
6	1,500
8	2,000
10	2,500

the manufacturer's protocol. The proportion of cells undergoing apoptosis (Annexin-positive/PI-negative cells and Annexin-positive/PI-positive cells) was evaluated using a fluorescence-activated cell sorting (FACS) system (FACScan; Beckman Coulter Cytomics FC500 Flow Cytometer, California, USA).

**Reverse transcription-quantitative polymerase chain reaction (RT-qPCR).** RNA was extracted from Eca109 and Eca109R60/2Gy cells using TRIzol reagent (Invitrogen, Thermo Fisher Scientific, Inc.) according to the manufacturer's protocol. Total RNA was reverse transcribed using a TaqMan Reverse Transcription kit (Takara Biotechnology Co., Ltd., Dalian, China). qPCR analyses were conducted using a Power SYBR Green kit (Takara Biotechnology Co., Ltd.). All analyses were performed according to the manufacturer's protocols. The expression of *HOTAIR*, *Snail*, E-cadherin, and  $\beta$ -catenin mRNA was determined by RT-qPCR using the following primer sequences: *HOTAIR*, forward, 5'-GCCTTCCCTGC TACTTGTG-3' and reverse, 5'-GGCTGGACCTTGTCTTCT ATG-3'; *Snail*, forward, 5'-TGACCTGTCTGCAAATGCTC-3' and reverse, 5'-CAGACCCTGGTTGCTTCAA-3'; E-cadherin, forward, 5'-AGCGTGTGTGACTGTGAAGG-3' and reverse, 5'-GCTGGCTCAAGTCAAAGTCC-3';  $\beta$ -catenin, forward, 5'-CCCACTAATGTCCAGCGTTT-3' and reverse, 5'-TGT CAGTTCAGGGATTGCAC-3'.  $\beta$ -actin was used as an internal control with the following primers: forward, 5'-CATCATGAA GTGTGACGTGGA-3' and reverse, 5'-ACATCTGCTGGA AGGTGGAC-3'. All RT-qPCR assays were performed on an ABI 7500 Fast Real-Time PCR system (Applied Biosystems, Thermo Fisher Scientific, Inc.). The total volume of the reaction mixture was 20  $\mu$ l (2  $\mu$ l reverse transcriptase, 0.8  $\mu$ l each forward and reverse template RNA primers, 6.4  $\mu$ l sterilized diethylpyrocarbonate water, and 10  $\mu$ l SYBR Select Master mix). The initialization step [uracil-DNA glycosylation (UDG) activation step] was set at 50°C for 2 min, followed by the AmpliTaq<sup>®</sup> DNA polymerase ultrapure (UP) activation step at 95°C for 2 min. The denaturation temperature was 95°C, held for 15 s, and annealing of primers for E-cadherin, *Snail*, and  $\beta$ -catenin was carried out at 55°C for 15 s. Extension was carried out at 72°C for 1 min. The annealing/extension steps for *HOTAIR* were carried out at 60°C for 1 min. The final three steps were run for 40 cycles. Expression levels of *HOTAIR*, *Snail*, E-cadherin, and  $\beta$ -catenin were normalized to those of  $\beta$ -actin. Their relative fold-changes in mRNA expression were calculated using the  $2^{-\Delta\Delta C_q}$  method (23).

**Western blot analysis.** Eca109 and Eca109R60/2Gy cells were lysed using radioimmunoprecipitation assay buffer (Beyotime Institute of Biotechnology, Beijing, China) supplemented with phenylmethylsulfonyl fluoride (Roche Diagnostics). From each sample, ~20  $\mu$ g protein was isolated, separated by SDS-PAGE on 8% gels, and transferred to 0.45-mm polyvinylidene fluoride membranes (EMD Millipore, Billerica, MA, USA). The membranes were blocked with 5% nonfat dry milk in Tris-buffered saline and Tween-20 (TBST; pH 7.6), and subsequently incubated overnight at 4°C with anti-SNAI1 (dilution, 1:1,500; H-130, sc-28199), anti-E-cadherin (dilution, 1:2,000; H-108, sc-7870) and anti- $\beta$ -catenin (dilution, 1:1,500; H-102, sc-7199) rabbit polyclonal antibodies, or with anti- $\beta$ -actin (dilution, 1:5,000; C4, sc-47778) mouse monoclonal antibodies (dilution, 1:5,000; all Santa Cruz Biotechnology, Inc., Dallas, TX, USA). Membranes were washed three times with TBST and incubated with horseradish peroxidase-labeled goat anti-rabbit immunoglobulin G (dilution, 1:200; ZB-2301; Zhongshan Golden Bridge Biotechnology Co., Ltd., Beijing, China) for 1 h at 22°C. Protein bands were detected using an enhanced chemiluminescent substrate (Pierce; Thermo Fisher Scientific, Inc.) and a ChemiDoc<sup>™</sup> MP imaging system (Bio-Rad Laboratories, Inc., Hercules, CA, USA). Relative protein expression levels are presented as the ratio of the OD x the area of each target to that of  $\beta$ -actin.

**Statistical analysis.** All data are presented as the mean  $\pm$  standard deviation and were analyzed using SPSS software v17.0 (SPSS, Inc., Chicago, IL, USA). Student's *t*-tests and analysis of variance (ANOVA) were used to analyze differences between the groups. Two-way ANOVA was employed to analyze the results of flow cytometry. The multitarget single hit model ( $S=1-[1-e^{-D/D_0}]^N$ ) was used to analyze and construct cell survival curves.  $P<0.05$  was considered to indicate a statistically significant difference.

## Results

**Effects of the radioresistant phenotype on cell proliferation.** Growth curves constructed using MTT assays demonstrated that in the initial 4 days, the growth rate of Eca109R60/2Gy cells was similar to that of Eca109 cells. However, after 5 days, Eca109R60/2Gy cells exhibited significantly increased proliferation compared with that of Eca109 cells ( $P<0.01$ ; Fig. 1).

**Effects of the radioresistant phenotype on colony-formation rates in ESCC cells.** Clone formation assays indicated that the colony-formation rate of Eca109R60/2Gy cells was significantly higher than that of Eca109 cells beginning on day 8, when cell colonies were visible by the naked eye, for all radiation doses (2 Gy, 0.767 $\pm$ 0.014 vs. 0.646 $\pm$ 0.012, respectively; 4 Gy, 0.652 $\pm$ 0.021 vs. 0.424 $\pm$ 0.027, respectively; 6 Gy, 0.494 $\pm$ 0.013 vs. 0.219 $\pm$ 0.011, respectively; 8 Gy, 0.287 $\pm$ 0.015 vs. 0.114 $\pm$ 0.024, respectively; and 10 Gy, 0.194 $\pm$ 0.005 vs. 0.063 $\pm$ 0.012, respectively;  $P<0.01$ ; Fig. 2).

Additionally, all radiobiological parameters were significantly higher in Eca109R60/2Gy cells than in the parental cell line. These parameters included mean lethal dose ( $D_0$ ; Eca109R60/2Gy vs. Eca109: 5.46 $\pm$ 0.28 Gy vs. 3.44 $\pm$ 0.19 Gy,

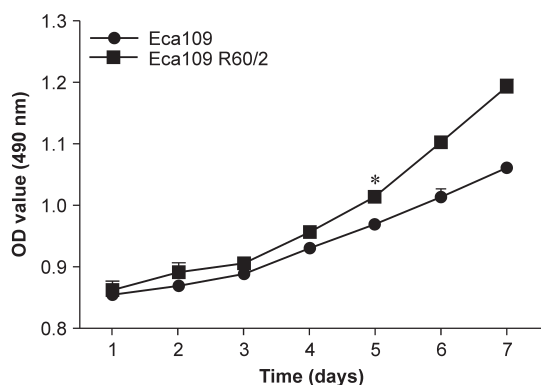


Figure 1. Cell proliferation curves of the Eca109R60/2Gy cells, compared with the Eca109 cells. \* $P < 0.01$ .

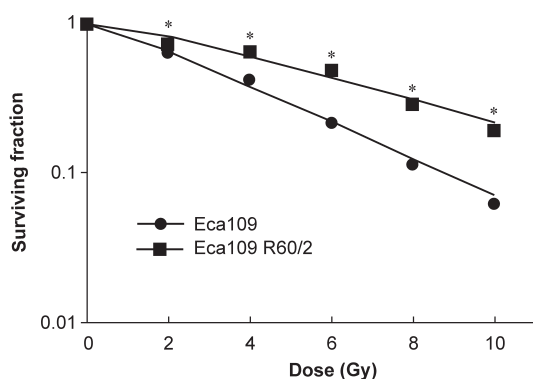


Figure 2. Cell survival curve of the Eca109 and Eca109R60/2Gy cells. \* $P < 0.01$ .

respectively;  $P < 0.01$ ), quasi field dose ( $D_q$ ; Eca109R60/2Gy vs. Eca109:  $2.49 \pm 0.59$  Gy vs.  $1.14 \pm 0.23$  Gy, respectively,  $P < 0.05$ ), and survival rate at 2 Gy ( $SF_2$ ; Eca109R60/2Gy vs. Eca109:  $0.77 \pm 0.01$  vs.  $0.65 \pm 0.01$ , respectively, ( $P < 0.01$ ; data not presented).

**Flow cytometry analysis.** There were significantly fewer Eca109R60/2Gy cells than Eca109 cells observed in the  $G_2/M$  phase ( $6.22 \pm 1.94\%$  vs.  $32.83 \pm 5.63\%$ , respectively) and significantly more Eca109R60/2Gy cells than Eca109 cells observed in the S-phase ( $54.95 \pm 3.60\%$  vs.  $30.27 \pm 1.72\%$ , respectively;  $P < 0.01$ ). There were no significant differences in  $G_1$  phase ( $38.83 \pm 1.74\%$  vs.  $36.97 \pm 4.29\%$ , respectively;  $P > 0.05$ ). Furthermore, the apoptosis rate in Eca109R60/2Gy cells was significantly lower than that in Eca109 cells ( $1.97 \pm 0.45\%$  vs.  $7.33 \pm 0.45\%$ , respectively;  $P < 0.0001$ ; Fig. 3).

**Effects of the radioresistant phenotype on the mRNA expression of HOTAIR and biomarkers of EMT and CSCs.** Expression levels of *HOTAIR* ( $3.00 \pm 0.62$  vs.  $1.00 \pm 0.00$ ;  $P = 0.0306$ ), *Snail* ( $3.02 \pm 0.14$  vs.  $1.00 \pm 0.00$ ;  $P = 0.0016$ ) and  $\beta$ -catenin ( $2.46 \pm 0.38$  vs.  $1.00 \pm 0.00$ ;  $P = 0.0220$ ) mRNAs were significantly increased in Eca109R60/2Gy cells compared with those in Eca109 cells (Fig. 4). By contrast, the mRNA expression level of *E-cadherin* in the Eca109R60/2Gy cells was significantly lower than in the Eca109 cells ( $0.41 \pm 0.08$  vs.  $1.00 \pm 0.00$ , respectively;  $P = 0.0061$ ; Fig. 4).

**Effects of the radioresistant phenotype on the protein expression of EMT/CSC markers.** Western blot analysis indicated that the levels of *SNAIL* and  $\beta$ -catenin were significantly higher in Eca109R60/2Gy cells than in the parental cell line ( $0.32 \pm 0.02$  vs.  $0.16 \pm 0.01$ ,  $P < 0.0001$ ; and  $0.11 \pm 0.01$  vs.  $0.07 \pm 0.00$ ,  $P = 0.0005$ , respectively; Fig. 5). In contrast, *E-cadherin* expression was significantly lower in Eca109R60/2Gy cells than in Eca109 cells ( $0.04 \pm 0.01$  vs.  $0.09 \pm 0.01$ ,  $P = 0.0020$ ; Fig. 5).

## Discussion

In this study, we examined the effects of the radioresistant phenotype on various cancer-associated parameters in ESCC cells. The results demonstrated that the radioresistant Eca109R60/2Gy cells exhibited increased proliferation, reduced apoptosis, and altered expression of *HOTAIR* and EMT/CSC markers compared with Eca109 cells. These data provide important insights into the mechanisms of radioresistance in ESCC.

In recent years, repeated low- to moderate-dose (2-6 Gy) and high-dose ( $\geq 8$  Gy) ionizing radiation methods have been employed to establish radioresistant cancer cells. As a result, different radioresistant cell models, including MGR2R glioma cells (24), nasopharyngeal carcinoma cells (25) and ESCC cells (26) have been generated using distinct exposure to ionizing radiation in order to improve our understanding of radioresistance mechanisms. In the present study, an Eca109R60/2Gy cell model was established from parental Eca109 cells by repeated exposure to 2 Gy ionizing radiation. MTT and colony formation assays indicated that proliferation and colony-formation rates were increased in Eca109R60/2Gy cells compared with that in Eca109 cells *in vitro*. Additionally, we demonstrated that Eca109R60/2Gy cells accumulated in the S phase and exhibited reduced rates of apoptosis compared with Eca109 cells. This is consistent with a previous study demonstrating that cells in  $G_2/M$  phase were the most sensitive to radiation, whereas cells in S phase were the most radioresistant (27). Thus, the results of the current study supported the notion that Eca109R60/2Gy cells are more radioresistant than their parental Eca109 cells and that this phenotype is closely associated with the accumulation of Eca109R60/2Gy cells in the S phase of the cell cycle.

Despite various studies investigating radioresistance in cancer, the specific mechanisms mediating radioresistance in cells remain unclear. Two explanations for radioresistance have been proposed. One is the heterogeneity of tumor cells, including the observation that the majority of radioresistant cancer cells are enriched during the course of irradiation (26). The second is that cancer cells adapt to irradiation and acquire radioresistance. The first explanation has recently been supported by a third explanation, the presence of CSCs; CSCs are defined as a subpopulation of tumor cells having both tumor-initiating ability and the ability to reconstitute the cellular heterogeneity typical of the original tumor, suggesting that resistance to conventional therapy may arise from CSCs rather than non-stem cells, despite apparent initial responses *in vivo* and *in vitro* (28,29); this may ultimately result in cancer development and recurrence (30,31).

Several studies have identified an association between CSCs and the EMT, with evidence suggesting that cells

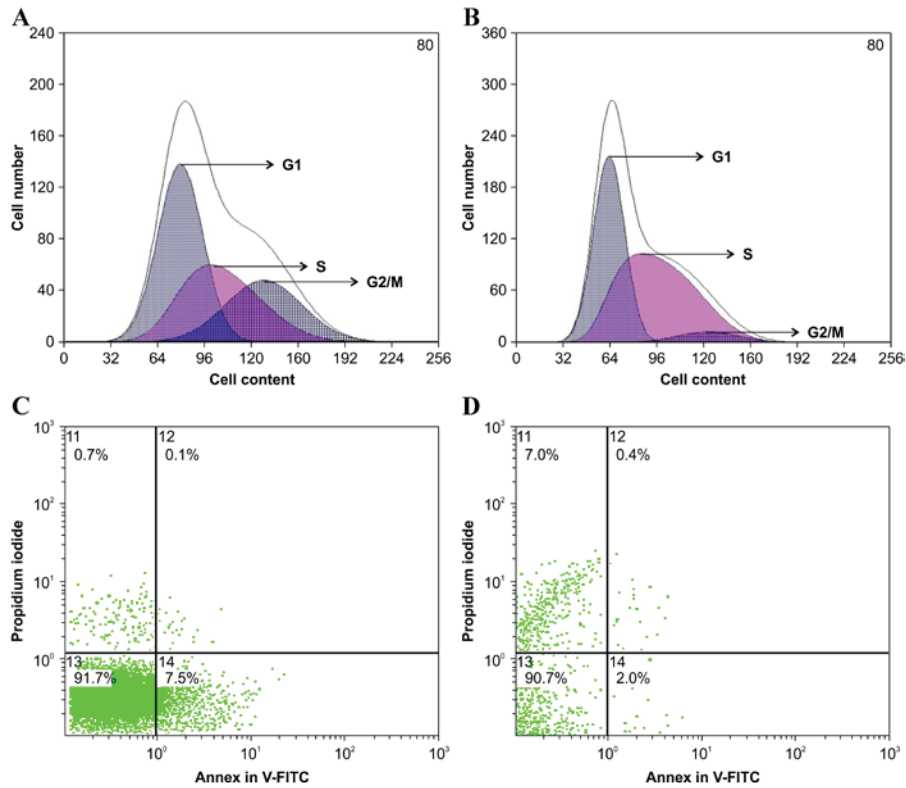


Figure 3. Comparison of cell cycle and apoptosis in Eca109 and Eca109R60/2Gy cells using flow cytometry. Cell cycle distribution for the (A) Eca109 and (B) Eca109R60/2Gy cells. Cell apoptosis in the (C) Eca109 cells and (D) Eca109R60/2Gy cells.

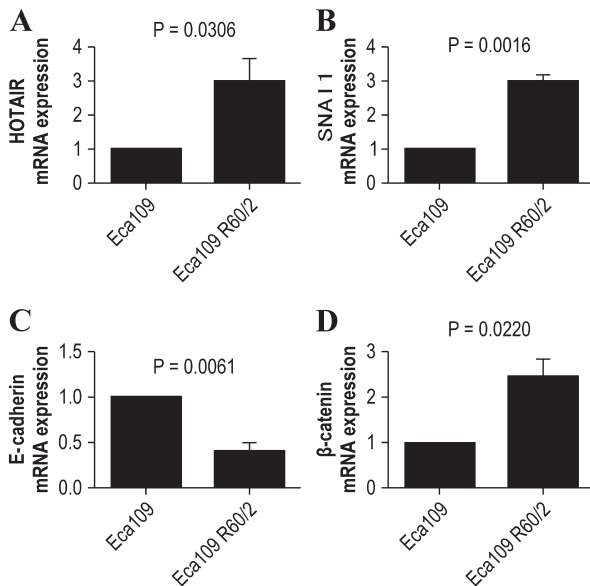


Figure 4. mRNA expression levels of (A) *HOTAIR*, (B) *Snail* (C) *E-cadherin*, (D)  $\beta$ -catenin, and epithelial mesenchymal transition/cancer stem cell markers in the Eca109 cells compared with the Eca109R60/2Gy cells. *HOTAIR*, HOX transcript antisense RNA.

undergoing the EMT acquire stem cell-like traits (32-34). Furthermore, CSCs exhibit a mesenchymal-like appearance in immortalized, non-tumorigenic mammary epithelial cells and breast cancer (33). The transcriptional repressor protein *SNAI1* triggers the EMT during embryonic development and fibrosis (35); this also occurs in carcinoma and is linked to

cancer cell invasion, chemo-/radioresistance, and the acquisition of CSC-like characteristics (35,36). This process is followed by the downregulation of *E-cadherin* (37), which is considered to mediate homotypic cell-cell adhesion and maintain normal morphology, epithelial cell polarity, and tissue structural integrity by binding to cytosolic  $\beta$ -catenin and forming the *E-cadherin*/ $\beta$ -catenin complex.  $\beta$ -Catenin is required for the EMT as it binds to *E-cadherin* and functions as a key molecule in the Wnt signaling pathway (37). The Wnt signaling pathway is crucial for stem cell survival, proliferation, differentiation, and chemo-/radioresistance (37,38) due to the action of Wnt inhibitory factor 1 (*WIF-1*), a critical inhibitor of the Wnt signaling pathway (39). Several studies have demonstrated that aberrant activation of the Wnt signaling pathway due to genetic and epigenetic alterations occurs in several types of cancer (39-42).

One of the possible underlying epigenetic alterations is DNA methylation in the promoter regions of *APC*, *Axin2*, and *WIF-1*. However, the mechanisms promoting DNA methylation of these factors are not clear. *Ge et al* (21) suggested that overexpression of *HOTAIR* activates the Wnt pathway by inhibiting *WIF-1* expression, leading to the accumulation of cytosolic  $\beta$ -catenin. This cytosolic (free)  $\beta$ -catenin is able to translocate into the nucleus and promote the transcription of genes that induce the EMT and enhance chemo-/radioresistance (37).

*HOTAIR* is highly expressed in breast, hepatic, colorectal, pancreatic, and lung cancer, and its expression is correlated with increased resistance to chemotherapy (13,17). Notably, the majority of tumors that are resistant to chemotherapy are also resistant to radiation therapy. Although direct supporting

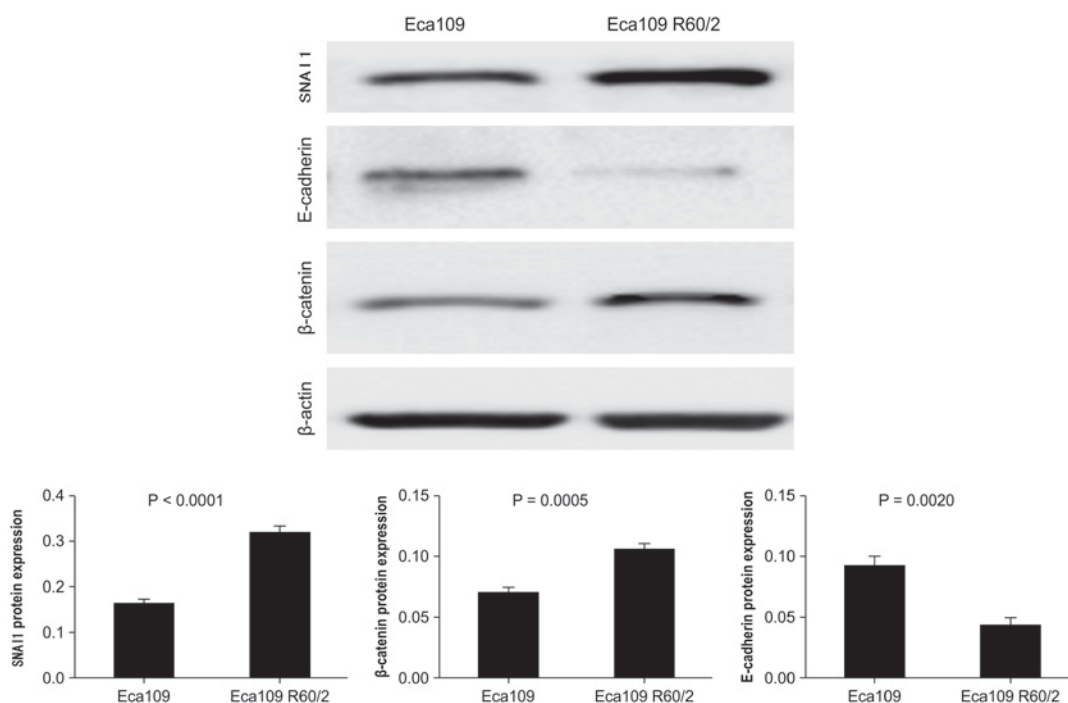


Figure 5. Western blot analysis indicating protein expression levels of epithelial-mesenchymal transition/cancer stem cell markers in Eca109 and Eca109R60/2Gy cells.

evidence is not available, *HOTAIR* is thought to participate in regulation of the EMT and CSCs, thereby promoting resistance to chemo- or radiotherapy. Moreover, *HOTAIR* regulates the levels of  $\beta$ -catenin (21), induces the expression of SNAI1, a marker of the mesenchymal phenotype, and inhibits the expression of E-cadherin, a marker of the epithelial phenotype (6,43). However, further studies are required to confirm whether *HOTAIR* and EMT/CSC biomarkers contribute to ESCC radioresistance.

In this study, we demonstrated that Eca109R60/2Gy cells exhibited increased radioresistance following radiation compared with that in parental Eca109 cells. Furthermore, the expression levels of *HOTAIR*, SNAI1, and  $\beta$ -catenin were significantly higher in Eca109R60/2Gy cells than in Eca109 cells. In contrast, E-cadherin expression was significantly lower in radioresistant cells, consistent with results of a previous study (26). Thus, in addition to increasing chemoresistance, *HOTAIR* may contribute to radioresistance by regulating the expression of EMT and CSC biomarkers, which mediate resistance to anticancer therapies.

In conclusion, the present study demonstrated that *HOTAIR* and EMT/CSCs may contribute to the development of resistance to radiation therapy in ESCC cells. However, the current study had several limitations. First, the expression levels of *HOTAIR* and EMT/CSC biomarkers were only detected using RT-qPCR and western blotting. Further studies utilizing techniques such as *in situ* hybridization and immunohistochemistry are necessary to confirm the results of the current study. Second, it remains unclear whether *HOTAIR* and EMT/CSCs collaboratively promote ESCC radioresistance. Finally, the present study did not fully elucidate the molecular mechanisms mediating the effects of these factors/pathways on radiation resistance in ESCC. Therefore, additional studies are required to address these issues.

## Acknowledgements

The present study was supported by the Natural Science Foundation of Xinjiang Uygur Autonomous Region (grant no. 2015211C115). The authors would like to thank Professor Huiwu Li of the Department of Biochemistry, Xinjiang Medical University (Urumqi, China) for supplying Eca109 ESCC cells.

## References

1. Ferlay J, Soerjomataram I, Dikshit R, Eser S, Mathers C, Rebelo M, Parkin DM, Forman D and Bray F: Cancer incidence and mortality worldwide: Sources, methods and major patterns in GLOBOCAN 2012. *Int J Cancer* 136: E359-E386, 2015.
2. Pakzad R, Mohammadian-Hafshejani A, Khosravi B, Soltani S, Pakzad I, Mohammadian M, Salehiniya H and Momenimovahed Z: The incidence and mortality of esophageal cancer and their relationship to development in Asia. *Ann Transl Med* 4: 29, 2016.
3. Lin Y, Totsuka Y, He Y, Kikuchi S, Qiao Y, Ueda J, Wei W, Inoue M and Tanaka H: Epidemiology of esophageal cancer in Japan and China. *J Epidemiol* 23: 233-242, 2013.
4. Cheng ML, Zhang L, Borok M, Chokunonga E, Dzamamala C, Korir A, Wabinga HR, Hiatt RA, Parkin DM and Van Loon K: The incidence of oesophageal cancer in Eastern Africa: Identification of a new geographic hot spot? *Cancer Epidemiol* 39: 143-149, 2015.
5. Ghiam AF, Spayne J and Lee J: Current challenges and future perspectives of radiotherapy for locally advanced breast cancer. *Curr Opin Support Palliat Care* 8: 46-52, 2014.
6. Gupta RA, Shah N, Wang KC, Kim J, Horlings HM, Wong DJ, Tsai MC, Hung T, Argani P, Rinn JL, *et al*: Long non-coding RNA *HOTAIR* reprograms chromatin state to promote cancer metastasis. *Nature* 464: 1071-1076, 2010.
7. Guttman M, Donaghey J, Carey BW, Garber M, Grenier JK, Munson G, Young G, Lucas AB, Ach R, Bruhn L, *et al*: lincRNAs act in the circuitry controlling pluripotency and differentiation. *Nature* 477: 295-300, 2011.
8. Khalil AM, Guttman M, Huarte M, Garber M, Raj A, Rivea Morales D, Thomas K, Presser A, Bernstein BE, van Oudenaarden A, *et al*: Many human large intergenic noncoding RNAs associate with chromatin-modifying complexes and affect gene expression. *Proc Natl Acad Sci USA* 106: 11667-11672, 2009.

9. Koerner MV, Pauler FM, Huang R and Barlow DP: The function of non-coding RNAs in genomic imprinting. *Development* 136: 1771-1783, 2009.
10. Kotake Y, Nakagawa T, Kitagawa K, Suzuki S, Liu N, Kitagawa M and Xiong Y: Long non-coding RNA ANRIL is required for the PRC2 recruitment to and silencing of p15 (INK4B) tumor suppressor gene. *Oncogene* 30:1956-1962, 2011.
11. Rinn JL, Kertesz M, Wang JK, Squazzo SL, Xu X, Bruggmann SA, Goodnough LH, Helms JA, Farnham PJ, Segal E and Chang HY: Functional demarcation of active and silent chromatin domains in human HOX loci by noncoding RNAs. *Cell* 129: 1311-1323, 2007.
12. Ishibashi M, Kogo R, Shibata K, Sawada G, Takahashi Y, Kurashige J, Akiyoshi S, Sasaki S, Iwaya T, Sudo T, *et al*: Clinical significance of the expression of long non-coding RNA HOTAIR in primary hepatocellular carcinoma. *Oncol Rep* 29: 946-950, 2013.
13. Yang Z, Zhou L, Wu LM, Lai MC, Xie HY, Zhang F and Zheng SS: Overexpression of long non-coding RNA HOTAIR predicts tumor recurrence in hepatocellular carcinoma patients following liver transplantation. *Ann Surg Oncol* 18: 1243-1250, 2011.
14. Kogo R, Shimamura T, Mimori K, Kawahara K, Imoto S, Sudo T, Tanaka F, Shibata K, Suzuki A, Komune S, *et al*: Long noncoding RNA HOTAIR regulates polycomb-dependent chromatin modification and is associated with poor prognosis in colorectal cancers. *Cancer Res* 71: 6320-6326, 2011.
15. Wu ZH, Wang XL, Tang HM, Jiang T, Chen J, Lu S, Qiu GQ, Peng ZH and Yan DW: Long non-coding RNA HOTAIR is a powerful predictor of metastasis and poor prognosis and is associated with epithelial-mesenchymal transition in colon cancer. *Oncol Rep* 32: 395-402, 2014.
16. Liu XH, Liu ZL, Sun M, Liu J, Wang Z and De W: The long non-coding RNA HOTAIR indicates a poor prognosis and promotes metastasis in non-small cell lung cancer. *BMC Cancer* 13: 464, 2013.
17. Liu Z, Sun M, Lu K, Liu J, Zhang M, Wu W, De W, Wang Z and Wang R: The long noncoding RNA HOTAIR contributes to cisplatin resistance of human lung adenocarcinoma cells via downregulation of p21(WAF1/CIP1) expression. *PLoS One* 8: e77293, 2013.
18. Xu Y, Li Y, Pang Y, Ling M, Shen L, Yang X, Zhang J, Zhou J, Wang X and Liu Q: EMT and stem cell-like properties associated with HIF-2 $\alpha$  are involved in arsenite-induced transformation of human bronchial epithelial cells. *PLoS One* 7: e37765, 2012.
19. Brabletz T, Jung A, Spaderna S, Hlubek F and Kirchner T: Opinion: Migrating cancer stem cells—an integrated concept of malignant tumour progression. *Nat Rev Cancer* 5: 744-749, 2005.
20. Yang J and Weinberg RA: Epithelial-mesenchymal transition: At the crossroads of development and tumor metastasis. *Dev Cell* 14: 818-829, 2008.
21. Ge XS, Ma HJ, Zheng XH, Ruan HL, Liao XY, Xue WQ, Chen YB, Zhang Y and Jia WH: HOTAIR, a prognostic factor in esophageal squamous cell carcinoma, inhibits WIF-1 expression and activates Wnt pathway. *Cancer Sci* 104: 1675-1682, 2013.
22. Kaufhold S and Bonavida B: Central role of Snail1 in the regulation of EMT and resistance in cancer: A target for therapeutic intervention. *J Exp Clin Cancer Res* 33: 62, 2014.
23. Xu ZY, Yu QM, Du YA, Yang LT, Dong RZ, Huang L, Yu PF and Cheng XD: Knockdown of long non-coding RNA HOTAIR suppresses tumor invasion and reverses epithelial-mesenchymal transition in gastric cancer. *Int J Biol Sci* 9: 587-597, 2013.
24. Cheng JJ, Hu Z, Xia YF and Chen ZP: Radioresistant subline of human glioma cell line MGR2R induced by repeated high dose X-ray irradiation. *Ai Zheng* 25: 45-50, 2006 (In Chinese).
25. Li G, Qiu Y, Su Z, Ren S, Liu C, Tian Y and Liu Y: Genome-wide analyses of radioresistance-associated miRNA expression profile in nasopharyngeal carcinoma using next generation deep sequencing. *PLoS One* 8: e84486, 2013.
26. Che SM, Zhang XZ, Liu XL, Chen X and Hou L: The radiosensitization effect of NS398 on esophageal cancer stem cell-like radioresistant cells. *Dis Esophagus* 24: 265-273, 2011.
27. Nicolay NH, Carter R, Hatch SB, Schultz N, Prevo R, McKenna WG, Helleday T and Sharma RA: Homologous recombination mediates S-phase-dependent radioresistance in cells deficient in DNA polymerase  $\epsilon$ . *Carcinogenesis* 33: 2026-2034, 2012.
28. Li X, Lewis MT, Huang J, Gutierrez C, Osborne CK, Wu MF, Hilsenbeck SG, Pavlick A, Zhang X, Chamness GC, *et al*: Intrinsic resistance of tumorigenic breast cancer cells to chemotherapy. *J Natl Cancer Inst* 100: 672-679, 2008.
29. Gupta PB, Onder TT, Jiang G, Tao K, Kuperwasser C, Weinberg RA and Lander ES: Identification of selective inhibitors of cancer stem cells by high-throughput screening. *Cell* 138: 645-659, 2009.
30. Charafe-Jauffret E, Ginestier C, Iovino F, Tarpin C, Diebel M, Esterni B, Houvenaeghel G, Extra JM, Bertucci F, Jacquemier J, *et al*: Aldehyde dehydrogenase 1-positive cancer stem cells mediate metastasis and poor clinical outcome in inflammatory breast cancer. *Clin Cancer Res* 16: 45-55, 2010.
31. Hermann PC, Huber SL, Herrler T, Aicher A, Ellwart JW, Guba M, Bruns CJ and Heeschen C: Distinct populations of cancer stem cells determine tumor growth and metastatic activity in human pancreatic cancer. *Cell Stem Cell* 1: 313-323, 2007.
32. Zhu LF, Hu Y, Yang CC, Xu XH, Ning TY, Wang ZL, Ye JH and Liu LK: Snail overexpression induces an epithelial to mesenchymal transition and cancer stem cell-like properties in SCC9 cells. *Lab Invest* 92: 744-752, 2012.
33. Mani SA, Guo W, Liao MJ, Eaton EN, Ayyanan A, Zhou AY, Brooks M, Reinhard F, Zhang CC, Shipitsin M, *et al*: The epithelial-mesenchymal transition generates cells with properties of stem cells. *Cell* 133: 704-715, 2008.
34. Biddle A, Liang X, Gammon L, Fazil B, Harper LJ, Emich H, Costea DE and Mackenzie IC: Cancer stem cells in squamous cell carcinoma switch between two distinct phenotypes that are preferentially migratory or proliferative. *Cancer Res* 71: 5317-5326, 2011.
35. Wu Y and Zhou BP: Snail: More than EMT. *Cell Adh Migr* 4: 199-203, 2010.
36. Polyak K and Weinberg RA: Transitions between epithelial and mesenchymal states: Acquisition of malignant and stem cell traits. *Nat Rev Cancer* 9: 265-273, 2009.
37. Wang Y, Shi J, Chai K, Ying X and Zhou BP: The role of Snail in EMT and tumorigenesis. *Curr Cancer Drug Targets* 13: 963-972, 2013.
38. Chen MS, Woodward WA, Behbod F, Peddibhotla S, Alfaro MP, Buchholz TA and Rosen JM: Wnt/beta-catenin mediates radiation resistance of Scal+ progenitors in an immortalized mammary gland cell line. *J Cell Sci* 120: 468-477, 2007.
39. Ramachandran I, Thavathiru E, Ramalingam S, Natarajan G, Mills WK, Benbrook DM, Zuna R, Lightfoot S, Reis A, Anant S and Queimado L: Wnt inhibitory factor 1 induces apoptosis and inhibits cervical cancer growth, invasion and angiogenesis in vivo. *Oncogene* 31: 2725-2737, 2012.
40. Lee BB, Lee EJ, Jung EH, Chun HK, Chang DK, Song SY, Park J and Kim DH: Aberrant methylation of APC, MGMT, RASSF2A, and Wif-1 genes in plasma as a biomarker for early detection of colorectal cancer. *Clin Cancer Res* 15: 6185-6191, 2009.
41. Taniguchi H, Yamamoto H, Hirata T, Miyamoto N, Oki M, Noshio K, Adachi Y, Endo T, Imai K and Shinomura Y: Frequent epigenetic inactivation of Wnt inhibitory factor-1 in human gastrointestinal cancers. *Oncogene* 24: 7946-7952, 2005.
42. Jiang Y, Li Z, Zheng S, Chen H, Zhao X, Gao W, Bi Z, You K, Wang Y, Li W, *et al*: The long non-coding RNA HOTAIR affects the radiosensitivity of pancreatic ductal adenocarcinoma by regulating the expression of Wnt inhibitory factor 1. *Tumor Biol* 37: 3957-3967, 2016.
43. Xu ZY, Yu QM, Du YA, Yang LT, Dong RZ, Huang L, Yu PF and Cheng XD: Knockdown of long non-coding RNA HOTAIR suppresses tumor invasion and reverses epithelial-mesenchymal transition in gastric cancer. *Int J Biol Sci* 9: 587-597, 2013.